Supplementary Information: Secondary flow in contour currents controls the formation of moat-drift contourite systems

Henriette Wilckens[1,2*], Joris T. Eggenhuisen[3], Pelle H. Adema[3], F. Javier Hernández-Molina[4], Ricardo Silva Jacinto[5], Elda Miramontes[1,2]

Supplementary Note 1: Forces that influence the experiment

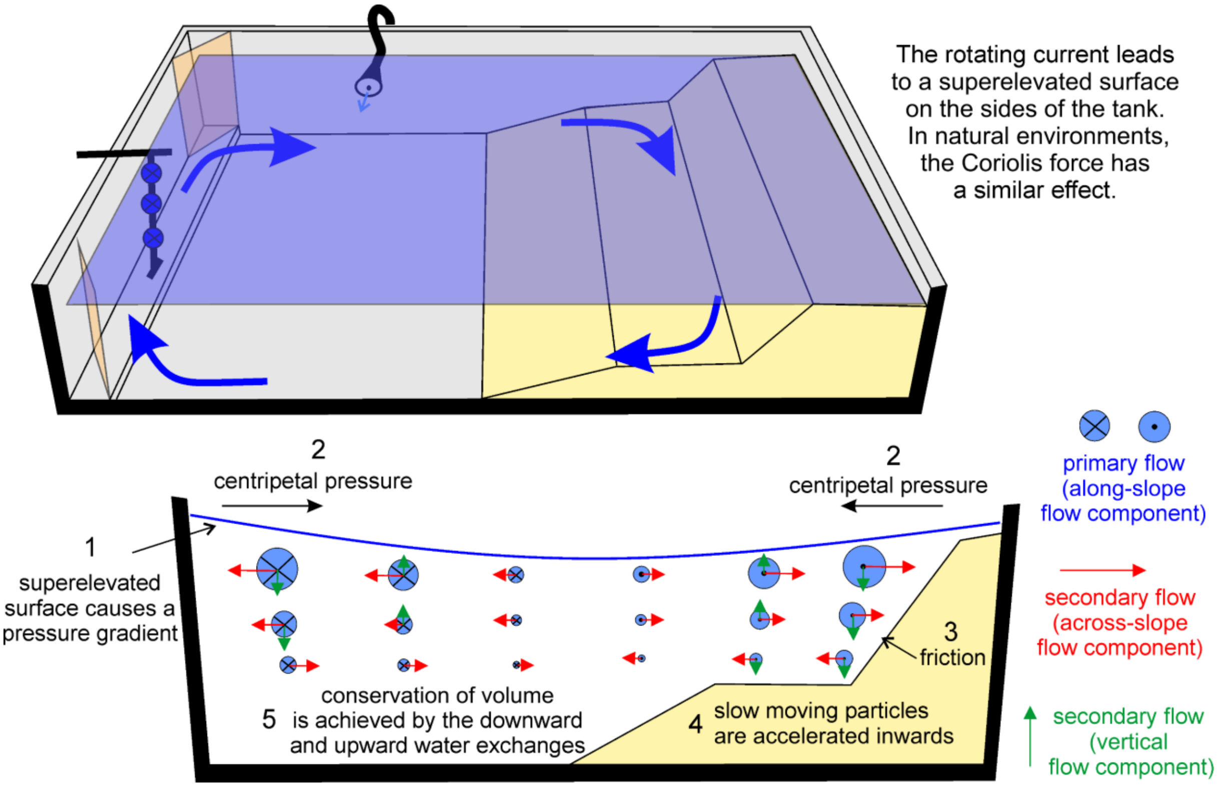

Fig. S1. Forces and currents that influence the experiments.

1. The rotation of the current leads to a superelevated surface[1]. In the natural environment, the Earth's rotation causing the Coriolis effect has a similar effect on the current[2]. The circular current in the flume tank has a higher speed away from the vortex center and becomes zero in the center of the vortex. Thus the current speed is higher near the slope and decreases over the terrace.
2. The superelevated surface causes an inward directed pressure gradient. The depth decreases above the slope and thus, the centrifugated and thinned water mass needs to increase its velocity in order to preserve centrifugal vorticity. Thus, the centripetal pressure gradient depends on the slope angle and current speed.
3. This centripetal pressure gradient is barotropic (constant in depth), but the velocity decreases towards the bed due to bed friction[2].
4. The slow flowing particles near the bed are accelerated inwards, while the fast flowing particles higher up in the water column are flowing outwards, resulting in a secondary flow near the bottom.
5. Conservation of volume is achieved by the downward and upward water exchanges between the lateral flows.

Supplementary Note 2: Sediment dynamics

The experiments were conducted with walnut shells with a grain size range of 200 – 450 µm and a density of 1350 kg/m^3. We used walnut shells due to their lower density compared to siliciclastic sediment. This allows the transport of walnut shells at lower velocities than siliciclastic sediment with the same grain size (Table S1). The bottom shear stress or bed shear stress τ to erode sediment depends on the velocity[3]:

$$\tau = p_{\mathrm{f}} u_*^2 \tag{1}$$

with seawater density p_{f} = 1000 kg/m^3 and friction velocity u_*. The friction velocity can be calculated assuming a logarithmic relation between the friction velocity and the variation of velocity with height, a von Kármán constant κ = 0.4 and z_0 = 0.0035 m as bottom roughness length[4] :

$$u_* = \frac{\kappa\, u(z)}{\ln \frac{z}{z_0}}, \tag{2}$$

where z = 20 cm is the distance from the bottom where the current velocity u(z) is measured. Sediment motion can be initiated when the maximum Shield parameter is higher than the critical bottom shear stresses[3]:

$$\frac{\tau}{g\,(p_{\mathrm{s}} - p_{\mathrm{f}})} d > \frac{0.3}{1 + (1.2 D_*)} + 0.055\left(1 - \mathrm{e}^{-0.02 D_*}\right), \tag{3}$$

with sediment density p_{s}= 2650 kg/m^3 for silt and 1350 kg/m^3 for walnut shells, diameter d, dimensionless grain sizer D_* and gravitational acceleration of g = 9.81 m/s. Dimensionless grain size D_* is calculated with:

$$D_* = \left(g \frac{\frac{p_{\mathrm{s}}}{p_{\mathrm{f}}} - 1}{\eta^2} \right)^{\frac{1}{3}} d\,, \tag{4}$$

where η = 1.0526 10^{-6} kg/m*s is the viscosity of water at 18°C. For the 11 cm/s, 16 cm/s and 18 cm/s current, the Shield parameter is 0.11, 0.22 and 0.28, respectively. According to the critical Shield parameter for motion initiation[3], the bottom shear stresses reach critical shear stresses (0.19 N/m^2 for silt and 0.05 N/m^2 for walnut shell) for the silt (sediment grain sizes d = 20 µm) and walnut shells (sediment grain sizes d = 325 µm) with a current velocity over 8 cm/s (measured 20 cm above the seafloor). Thus, we are using the walnut shell as an analog for silt because they are transported as bedload with similar speeds. The advantage of the coarse walnut shell over the fine silt is that it settles faster because according to Stokes' law the grain size goes into the settling velocity quadratic and the density only linear. This allows us to run the experiments in a smaller setup. The settling velocity is calculated with Stoke's law:

$$w_{\mathrm{s}} = \frac{p_{\mathrm{s}} - p_{\mathrm{f}}}{18\eta} d^2 g \tag{5}$$

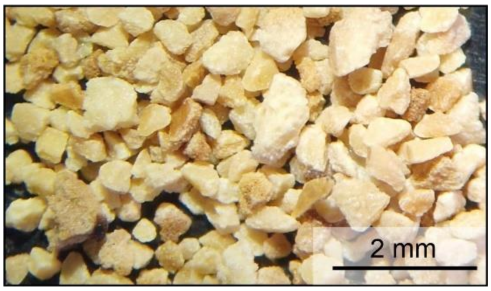

Fig. S2. Microscope photo of crushed walnut shells.

For silt with a diameter d = 20 µm and a density p_s = 2650 kg/m^3 the settling velocity is only 0.034 cm/s. For walnut shells with a diameter d = 325 µm and a density p_s = 1350 kg/m^3 the settling velocity is 1.914 cm/s. Stoke's law assumes spherical particles and the walnut shells are only roughly spherical (Fig. S2). Thus the calculation only gives a very rough estimate of the settling velocity.

Table S1: Summary of calculated sediment dynamics parameters.

	Current velocity 11cm/s	Current velocity 16cm/s	Current velocity 18cm/s
Sediment settling velocity (w_s)	1.9 cm/s	1.9 cm/s	1.9 cm/s
Friction velocity or flow shear velocity (u_*)	1.1 cm/s	1.6 cm/s	1.8 cm/s
Shields Parameter or non-dimensional bed shear stress	0.11	0.22	0.28
Critical threshold	0.05	0.05	0.05

With d50 = 325 µm, density 1000 kg/m^3 for water and 1350 kg/m^3 for walnut shell.

Supplementary Note 3: Comparison of the natural environment and flume tank moat-drift systems

The parameters of the moat-drift system in the flume tank are in a comparable order as those from the natural system. However, they are more similar to the maximum slope angle, aspect ratio and drift angle. These higher slope angles are found around topographic obstacles like seamounts[5]. But also at continental sedimentary margins, slope angles of 15° have been measured.

Table S2: Comparison of the natural environment and flume tank moat-drift systems. Values for the natural environment are taken from[5]

	Slope angle [°]		Moat aspect ratio		Drift angle [°]	
	Flume tank	Ocean	Flume tank	Ocean	Flume tank	Ocean
Minimum	18	0.3	0.02	0.001	4	0.2
Average	22	6	0.06	0.022	9.4	3
Maximum	26	25	0.09	0.1	15	17

Supplementary References

1 Childs, P. (2010). Rotating flow. Elsevier.
2 Özsoy, E. (2020). Geophysical Fluid Dynamics I. Springer.
3 Soulsby, R., & Whitehouse, R., (1997). Threshold of sediment motion in coastal environments, Pacific Coasts and Ports' 97: Proceedings of the 13th Australasian Coastal and Ocean Engineering Conference and the 6th Australasian Port and Harbour Conference; Volume 1. Centre for Advanced Engineering, University of Canterbury, p. 145.
4 Schlichting, H., (1962). Boundary Layer Theory, 6th ed. McGraw-Hill, New York. 744 pp.

5 Wilckens, H., Schwenk, T., Lüdmann, T., Betzler, C., Zhang, W., Chen, W., Hernández-Molina, F.J., Lefebvre, A., Cattaneo, A., Spiess, V., & Miramontes, E., (2023). Factors controlling the morphology and internal sediment architecture of moats and their associated contourite drifts. Sedimentology, 70, 1472–1495.

6 Miramontes, E., Cattaneo, A., Jouet, G., Thereau, E., Thomas, Y., Rovere, M., Cauquil, E., & Trincardi, F., (2016). The Pianosa contourite depositional system (northern Tyrrhenian Sea): drift morphology and Plio-Quaternary stratigraphic evolution. Marine Geology, 378, 20–42.